



---

RESEARCH ARTICLE

---

A PLATFORM FOR ULTRA-COLD EXTERNAL CAVITY DIODE LASERS

İbrahim KÜÇÜKKARA<sup>1,2</sup> , Barış POLAT<sup>2</sup> 

<sup>1</sup> Department of Physics, Faculty of Science and Literature, Mersin University, Mersin, Turkey

<sup>2</sup> Department of Nanotechnology and Advanced Materials, Graduate School of Natural and Applied Sciences, Mersin University, Mersin, Turkey

ABSTRACT

Tunable lasers one of the important tool of atomic manipulation and quantum interference and modern spectroscopy. However classical tunable coherence light sources such as dye lasers or optical parametric oscillators are expensive and difficult to maintain and operate. Diode lasers may be good alternative to those well-known tunable lasers with some modification such as constructing external cavity and with a good thermal stabilisation. Also many available commercial diode lasers may not cover the atomic absorption lines. To overcome those problems, we design and constructed a platform for ultra-cold tuneable external cavity diode laser system working at -50 °C and under rough vacuum (at 28mBar). Temperature tuning capability of the system was examined utilizing a 658nm (AlGaInP) single mode laser diode. With the system designed the temperature dependent tuning range was expended to almost two fold (down to 650nm at -50°C) while halving the bandwidth (less than 7MHz) regarding to its room temperature (at 25 °C) performances. As opposed to water cooling and very thick isolation that makes the laser system impractical, in our design heat dissipation was achieved by air cooling taking advantages of ease of operation, less complicated system, compactness with safety for the optical and electronic devices used. A theoretical procedure is also presented to calculate thermal control parameters including heat transfer rate, thermal isolation and heat dissipation of the system.

**Keywords:** Tuneable lasers, External cavity diode lasers, Ultra-cold platform

---

1. INTRODUCTION

Semiconductor laser diodes have found widespread use in the diverse fields of industrial and scientific applications. They increasingly gain importance since they have great advantages over the most other types of lasers due to their compactness, larger gain curve capability, ease of use, low cost and high electrical to laser power conversion efficiency [1-2]. If a tuneable diode laser is in question, its spectral characteristics (mainly spectral purity) and continuous tuning range are the primary interests for many atomic physics related experiments and applications.

A narrow linewidth tuneable laser is the principle device for use in: metrology and atomic clocks [3], laser cooling and trapping [4-5], Electromagnetically Induced Transparency (EIT) and some other phenomenon based on quantum interference effects [6] and high resolution spectroscopy experiments [7]. However, for many applications, a solitary diode laser cannot meet the requirements due to its larger bandwidth, beam divergence, poor frequency stability and sensitivity to back reflections. Despite those drawbacks spectral performance of a laser diode can be significantly improved by constructing an external cavity placing a Frequency Selection Element (FSE) in front of the diode output. With this optical feedback technique, some portions of the beam reflected back into the laser diode by forcing the internal cavity lasing at the reflected wavelength. An external cavity diode laser (ECDL) system shows much better spectral purity than the laser running without feedback.

The first semiconductor laser diode was operated at the room temperature is in the year of 1970. The meaning of “the room temperature” is 25 °C that is the standard test and operation temperature of laser

---

\*Corresponding Author: [ikucukkara@mersin.edu.tr](mailto:ikucukkara@mersin.edu.tr)

Received: 23.12.2019 Published: 29.06.2021

diodes accepted in laser field and by the most laser manufacturers. Two years later quantum-well lasers came with lower threshold current and much more efficiently runs at room temperature. This type of diode laser continued to develop throughout the 1970s and became technologically sound in the first half of the 1980s and began to be used in practical applications. Fleming and Moradian was the first group investigating bandwidth characteristics of the ECDL lasers in detail [8]. In 1990s ECDL systems were the essential tool for atomic physics and spectroscopy because of their wavelength tuning characteristics and narrower linewidth output. Several groups have investigated the ECDL systems to improve its critical weaknesses and they published so many reviews and articles including; simplicity of construction and compactness [9], coupling efficiency [10] and optical feedback [11], frequency selection with band-pass filters [12], transmission gratings [13], Volume Phase Holographic Grating (VPHG) [14], spectral characteristic [15] and line-width measurement [16], laser wavelength control [17] and increasing the mod-hop free running range [18].

In the ECDL based systems the most common external cavity type, is the Littrow configuration in which the first order diffracted beam is reflected back to the laser by a FSE. Many ECDLs are based on reflective diffraction grating as FSE in the Littrow configuration because of its simplicity and ease of use [see 9]. Due to stronger feedback intensity this method substantially reduces the linewidth and stabilises the intensity of output beam while allowing course and fine wavelength tuning. But such a simple design has important disadvantages. First of all, during the wavelength scanning process, the output beam deflects from its original position and secondly the mod-hop free tuning range is limited. A transmission diffraction grating is a good alternative since it removes the beam directional variation problem. But this is gained at the expense of weaker back reflection leading to reduced stability and larger linewidth. Along with stronger feedback, longer cavity length reduces the linewidth. But for a maximum mod-hop free scan range, shorter cavity is essential [18]. Also using separate optical elements for feedback and frequency selection (e.g. mirror and interference filter) is possible but it increases the complexity of the mode-hop free tuning [14]. Consequently, for an ECDL system with narrower linewidth and wider mod-hop free tuning range are the most desirable features but it is not possible to handle both usefulness at the same time. Moreover, for a transmission frequency element the interplay between narrow linewidth and mod-hope free tuning range makes the solution more complicated. Another alternative is to run the laser diode at the possible lowest temperature. This will reduce the quantum noises in the laser diode bringing narrower linewidth without sacrificing mod-hope free tuning range [15].

Laser diodes may have large manufacturing tolerances. Therefore, they may behave differently, in terms of wavelength, power, threshold, beam waist size, beam divergence, beam pointing. Some of those large tolerances can be utilised improving the performances of the laser. Today semiconductor laser diodes are used in various fields and mostly their production depends on the telecommunication industry. Correspondingly, their mass production brings the prices down. However, readily available, low cost and mass produced laser diodes covering the wavelength range from  $395\text{nm}$  to  $1570\text{nm}$  do not have a continuous tuning line. Particularly, for laser related spectroscopy incomplete spectral coverage is being one of the major drawbacks.

In order to extend the tuning range of an ECDL system, there are numbers of designs running the laser diodes far from the room temperature down to  $-45^{\circ}\text{C}$  [19, 20, 21]. The list of ultra-cold ECDL system designed is given in Table 1. Mainly working well below the room temperature requires very thick isolation for reaching and keeping it in an efficient way in a reasonable time interval. Also nitrogen must be pumped in the cavity chamber to eliminate the dump causing ice that blocks some of the laser output power. Moreover, reaching such a low temperature produces a substantial amount of heat to be removed from the laser system. Therefore, as a straightforward approach a water cooling system is to be employed to evacuate the heat dissipated.

**Table 1.** The list of ultra-cold ECDL designs

Ref.	Isolation/ Cavity Media	Exhaust Heat Management	Minimum Temperature (°C)
[4]	Vacuum/Vacuum	Water cooling	-20
[5]	Metal Lid/ Nitrogen	Water cooling	-31
[19]	Polystyrene/Atmospheric	Air Cooling	-45
[20]	Plexiglas/Polystyrene	Water cooling	-31
[21]	Vacuum/Vacuum	Water cooling	-64

Thick isolation restricts working space for optics and opto-mechanic components. Using water cooling makes the system complicated and very risky for optics and electronic components in case of water leakage. Clearly, all the disadvantages restrict low temperature laser system's practical use and operation. Whereas, running an ECDL system at well below the room temperature condition bring some advantageous. The potential benefits are: 1) it is possible to extend the rough tuning range can be two fold or more, 2) due to the reduced quantum noises (mainly spontaneous emission causes phase noise) linewidth of the output beam can be reduced up to three fold and there will be a substantial reduction of the power fluctuations; 3) very low lasing threshold current meaning that higher electrical-to-optical efficiency; 4) no need longer external cavity that potentially causing mechanical noise because laser diode has much narrower linewidth than that of being at the room temperature; 5) A low operating temperature generally lengthens the life expectancy. The main life lime limiting factor of a laser diode is operating temperature that is directly proportional to the current applied. In most ECDL applications laser diode is operated maximum current due to strong optical feedback for narrower linewidth and output power stability.

Generally, a cooling system is the necessary part of all types of lasers and it is arranged such that not only removing the heat dissipated from the device but also keeping the laser cavity temperature at a fixed point (usually at about room temperature). Thermal management of a laser system is a critical issue for keeping of the beam quality and the life time of the components at a desired level. Thermal control of semiconductor diode lasers is much more critical than that of the any other laser type because they are exposed to high heat loads regarding of their compact size. Typically, a lasing media as small as  $500\text{-}100\text{-}8\mu\text{m}$  in size also causes frequency noise problems, due to increased spontaneous emission in the cavity, leading to linewidth enhancement. Relatedly, their short cavity length, causes poor wavelength control, wider linewidth and instability. Also their optical efficiencies are highly temperature dependent, so precise temperature control is necessary. A typical temperature versus wavelength  $d\lambda/dT$  slope is in between  $-0.2\text{nm/K}$  and  $-0.3\text{nm/K}$  and lasing frequency depends on temperature and injection current; the sensitivities are typically  $30\text{GHz/K}$  and  $3\text{MHz}/\mu\text{A}$  respectively.

When the driving current is above the specific threshold, the output power of laser diode is in a linear relationship with the current applied. Also for stable oscillations in the laser cavity, a higher optical feedback is essential. Therefore, higher driving current is needed to maintain a constant output power level. However, the threshold current of the laser increases with the increasing temperature. Consequently, for a diode laser operation with stable power, precise thermal control and lower temperature environment produces more satisfactory result.

For a tuneable laser diode, if frequency stability is desired, the short cavity length is being problematic due to short photon lifetime in the cavity. The problem can be overcome by an additional external frequency-selective cavity element that allows control of the operating wavelength over a few nanometres range, with *sub-MHz* linewidth stability. The external cavity is formed by an FSE and the diode rear facet, and because the feedback from the FSE is generally greater than that of the front facet, the external cavity determines the lasing wavelength. Therefore, the spectral performance of an ECDL is strongly dependent on the external environment. Particularly, stability of the laser oscillation is

effected by acoustic disturbances in the air gap of the external cavity. And also depending on the humidity, low temperatures may induce condensation on the diode and collimation lens.

Mostly, thermal management of a laser takes advantage of convection, conduction and radiation to move the heat away from the heat generator in an efficient way. In general, available cooling systems fall into the following categories: liquid pumped systems, heat pipes, heat sinks, thermoelectric coolers (TECs). Advanced cooling systems incorporate liquid cooling and cryogenic systems. These systems are often large and bulky, and can easily break down due to a large number of moving parts. Usually, the solutions of cooling system for diode lasers working under well below room temperature, typically, use liquid cooling approaches to maintain the diode temperature. However, low working temperatures and liquid environments can easily introduce moisture into the system or neighbouring components which lead to detrimental thermal or electrical conditions. Moreover, conventionally considering the laser operation at low temperatures require thicker isolation that will occupy more space.

Regarding ultra-cold ECDL, the system must specifically deliver the following advantages over the other designs: 1) the system must be space efficient meaning that less isolation so enough room for the optics and the other space components; 2) with the exception of a fan, system has no moving parts. Existing systems often require liquid cooling pumps, fans, and other components which greatly reduce the working lifetime of the system; 3) the system can be easily controlled and adjusted by a variable DC source; 4) less moving parts means that maintaining the system is quite easy; 5) the cavity must be hermitically sealed for addition suppression of environmental fluctuations and drift. So that the laser is stable robust, and relatively in sensitive to acoustic disturbances; 6) no humidity condensation on the laser and other optical components.

In this article, we describe design and construction of a vacuum ultra-cold ECDL system. In the designing stage, our calculations on the heat loads and heat transfer rates of the system showed that at the room temperature, under 28mBar rough vacuum and without thermal isolation it is possible to get the laser diode case temperature  $-50^{\circ}\text{C}$  (or even lower). This modest vacuum good enough to reduce the damp inside the system down to %1 relative humidity. Moreover, it makes the laser operation easier by eliminating the nitrogen requirements of the system to reduce the damp in the vacuum chamber. Also the calculations showed that generated heat can be evacuated by only air cooling without any need for a water cooling system. The vacuum chamber that surrounded the ECDL system was constructed on a large aluminium heatsink. In the design there is enough room establishing a longer external cavity and for other optics required. The room inside vacuum chamber allows installing larger opto-mechanic components. Using a transmission diffraction grating in the Littrow geometry eliminates beam divergence during the scanning process. But, transmission grating causes lager linewidth due to weaker back reflection. This can be compensated by making cavity longer at the expense of reduced mod-hop free scan range. However, another alternative for the linewidth reduction that may be running the laser at lower temperatures. Our system runs  $75^{\circ}\text{C}$  below the room temperature (223K) that approximately reduces the laser bandwidth two fold. And also such a low temperature brings the lasing threshold current to lower range meaning that higher electrical-to-optical efficiency.

## 2. MATERIALS AND METHODS

The ECDL system designed is shown in (Figure 1). Components of the system were constructed on a  $300\times 200\times 83\text{mm}^3$  commercially available heat sink. It is made of 6063 series casting aluminium with  $200\text{Wm}^{-1}\text{K}^{-1}$  thermal conductivity. The thickness of its top plate is 25mm. The laser housing, the acrylic cover and the optic mounts were fitted onto the plate. The housing was machined from a  $70\times 30\times 40\text{mm}^3$  copper bar accommodating a laser tube that contains a laser diode and a collimating lens.

The laser housing can readily be cooled down to  $-50^{\circ}\text{C}$  by three Thermoelectric Coolers (TEC) fitted in cascade form. The air cooling of the heatsink was managed by two 120mm cooling fans and they were

fixed under the platform flaps. The acrylic vacuum cover was also designed and assembled in our laboratory. It is made of 15mm thick acrylic plates. The pieces were adhered with the aid of chloroform that it is a good solvent for acrylic. The final dimensions of the cover are of 250x180x100mm<sup>3</sup>.

The air inside the chamber is evacuated down to 28mBar by a small diaphragm type vacuum pump with the power of 12W (12V and 1A). From one side of the heat sink plate, two tapped holes opening the plate surface are placed. The holes are 10mm in diameter one of which is for evacuating the air and the other one is for fitting the signal and power cables. Both of them were sealed with silicon sealer for tight vacuum. A vacuum sealing is cut so as to fit bottom of acrylic lid and is located between the lid and heat sink plate. It is a silicon rubber with 15mm wide and 3mm thick.

Modifications on the heat sink were minimal. The surface of the platform was used as a mounting surface for the components of the system. In order to keep the acrylic lid firm on the platform a 5mm depth channel was milled that was exactly same size of the bottom of the lid. Between the lid and the channel, sealing rubber was fitted. Such design helps keeping the lid and rubber sealing tightly in its original place and so it eliminates the need for screws and mechanical modification that saves labour and costs. It is possible to get down to 28mBar in a few minutes keeping the tight vacuum almost one week.

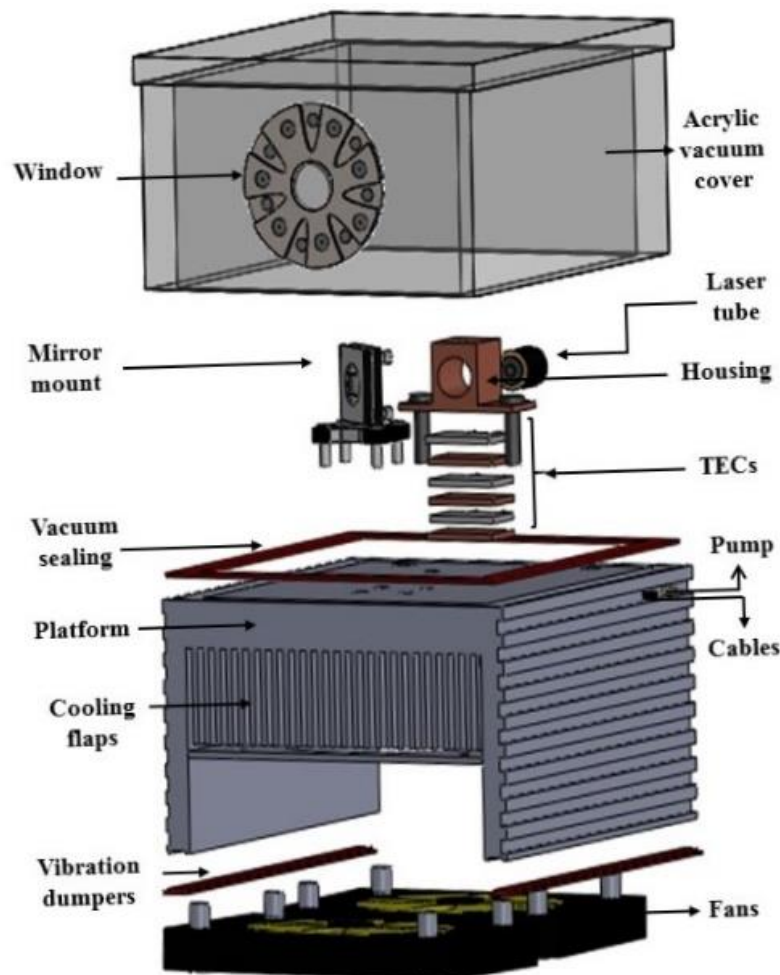


Figure 1. Schematic depiction of the experimental system

A good thermal conductivity is essential for a larger tuning range and for a stable laser output. For a precise thermal control, the housing was designed and machined from a copper block. It has conducting surface area 40x40mm<sup>2</sup>. A diode laser tube (Thorlabs LT230P) was fitted into the housing. The thermal

control of the laser diode a thermal sensor was fixed in a hole drilled into the housing just underneath the tube. The TECs were located in the cascade form down below the laser housing. Highly polished 5mm thick copper plates were located between the TECs to ensure evenly distributed heat conductivity.

To minimise the unwanted back-reflections and so increasing the external cavity stability, an anti-reflection coated vacuum wedged window was preferred (Thorlabs VPCHW42-B). The 658nm beam delivery can also be achieved by a single mod fibre cable with collimation lenses (Thorlabs P1-630P-FC-1 and F810FC-635). We have seen that using a transmission grating-fibre cable combination may be a useful design for our vacuum based system.

### 2.1. Designation of the Thermal Control System

The laser housing was cooled by the TECs with three different cooling capacities that they were arranged in the cascade form. The TECs combination was decided by examining various numbers of TECs. We found that for the maximum temperature difference, the top TEC had to have utmost one third of cooling capacity with respect to bottom ones. The TECs had limited COP values (Coefficient of Performance) which was about 0.614 for our case. For the maximum temperature difference the TECs were operated at  $0.5I_{max}$  which are their operating maximum current. Regarding these restrictions, we have an empiric formulation for cooling capacities of each TEC. That is  $P_1 \geq 3(P_2 + P_3)$ ,  $P_2 \geq 3P_3$  and  $P_1 \geq 12P_3$  where  $P_1$ ,  $P_2$  and  $P_3$  represent the lower, middle and upper TECs respectively. Specs of the TECs used is given in Table 2. Maximum cooling capacity  $Q_{max}$  in the table are applied currents  $I_{max}$ , voltages  $V_{max}$  and at the temperature differences between hot and cold surfaces of the TECs will be equal to zero ( $\Delta T = 0$ ). Also for the maximum temperature difference ( $\Delta T_{max}$ ) at  $I_{max}$  and  $V_{max}$  maximum cooling capacity will be equal to zero ( $Q_{max} = 0$ ). This applies for all TECs used. The number of couples of the TECs identify the maximum voltages applied, for each couple the maximum voltage is about 0.125V so for 288 couples  $V_{max}$  is about 36V.

**Table 2.** Table of specs of the thermoelectric modules used

TECs	P <sub>1</sub>	P <sub>2</sub>	P <sub>3</sub>
<b>Number of Couples</b>	288	287	127
<b>V<sub>max</sub> (Volt)</b>	36.0	35.9	15.4
<b>I<sub>max</sub> (Amp)</b>	15.4	3.9	3.8
<b>Q<sub>max</sub> (Watt)</b>	340	85.6	36
<b>ΔT<sub>max</sub>=(T<sub>cold</sub>-T<sub>hot</sub>) °C</b>	68	74	74
<b>COP (=I<sub>max</sub>x V<sub>max</sub> /</b>	0.614	0.618	0.615
<b>R (ohm)</b>	1.97± 0.05	8.1± 0.05	3.6± 0.05
<b>Dimensions (mm)</b>	50x50x3.6	40x40x3.6	30x30x3.6

Due to detrimental effect of the excess current applied on the temperature difference, the lower ( $P_1$ ) and the middle ( $P_2$ ) TECs are connected in parallel. This type of electrical connection allows to control both of the TECs and to identify optimum current for maximum temperature difference via only one power supply. The power supply M10-QS3020 drives the bottom and middle TECs  $P_1$  and  $P_2$  respectively. The upper TEC is driven by a current controller unit managing temperature via the thermal sensor. The controller ITC-510 drives both the upper TEC  $P_3$  and diode laser currents. Specifications of the power supply and the controller unit is given in Table 3.

**Table 3.** Table of specs of the power supplies used for the laser system

	Power Supply	Controller
<b>Model</b>	M10-QS3020	ITC-510
<b>V (V)</b>	0-30	0-8
<b>I (A)</b>	0-20	0-4
<b>Power (W)</b>	600	32
<b>V<sub>accu.</sub> (mV)</b>	±10	±0.4
<b>I<sub>accu.</sub> (mA)</b>	±10	±0.4
<b>T<sub>range.</sub> (°C)</b>	NA	-
<b>T<sub>accu.</sub> (°C)</b>	NA	±0.1

## 2.2. Laser Cavity Configuration

The external cavity configuration of the system is given in (Figure 2). Usually in an ECDL system frequency selection is managed by a reflection diffraction grating in the Littrow configuration due to its simplicity. But, for this type of configuration, during the tuning process, the beam deviation is a well-known problem. Using the transmission grating the beam divergence is eliminated at the expense of larger bandwidth due to weaker feedback reflection. It is possible to compensate bandwidth enlargements by increasing the external cavity length at the expense of reduction on the mod-hop free scan range. The frequency selection for the 652nm laser was achieved by a transmission grating (Thorlabs GTU13-12). The grating was fitted into a piezoelectric kinematic mirror mount (Thorlabs PZ631B/M) that is fitted onto a rotational manual rotational stage (Thorlabs RP01/M). In our case the distance between the grating and the laser diode is 35mm that is relatively shorter regarding a transmission FSE. This is because the laser diode was operated at -50°C and that allows us almost two-fold linewidth reduction. This compensated the bandwidth enlargements due to the weaker back reflection in to the cavity. The configuration allowed us to find the Littrow angle manually and fix it with a rotation locking screw placed in the rotational stage. Such design allows re-adjusting the Littrow angle of the grating when it is needed.

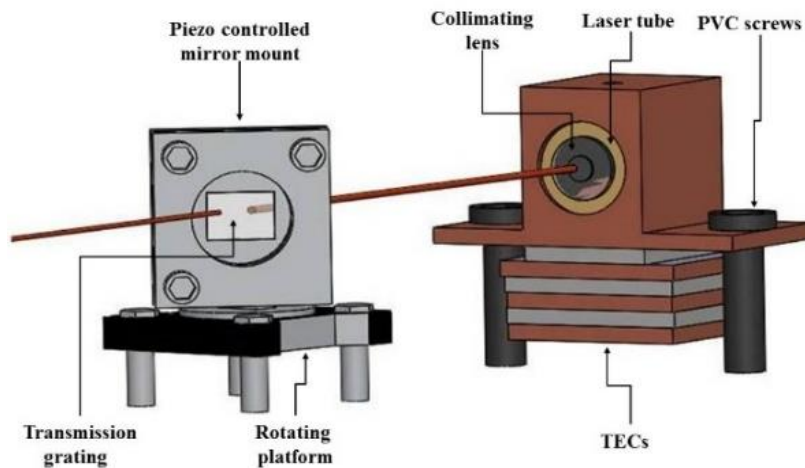


**Figure 2.** The design of external cavity of the diode laser

### 2.3. Mathematical Simulation of the Heat Transfer

The cooling capacities of the TEC modules were decided regarding the total heat load on the system  $Q_T$  that includes  $Q_{mass}$  representing the heat to be transferred from the copper housing and  $Q_{load}$  is active and passive heat loads.

$$Q_T = Q_{mass} + Q_{load} \quad (1)$$

$Q_{mass}$  Represents the heat to be transferred from the laser housing and can be calculated via Newton's law of cooling

$$Q_{mass} = mc_p \Delta T / t \quad (2)$$

where  $m$  is the total mass,  $c_p$  is specific heat capacity of copper,  $\Delta T$  is the difference between initial and final temperatures,  $t$  is the time for reaching to the coldest point of the laser housing.

$Q_{load}$  can be described as

$$Q_{load} = Q_{conv} + Q_{cond} + Q_{rad} + Q_{act} \quad (3)$$

here first three term is regarded as passive and the last term active heat loads. Passive heat load on the system comes from heat flow due to convection ( $Q_{conv}$ ), radiation ( $Q_{rad}$ ) and conduction ( $Q_{cond}$ ). They can be expressed as sets of equations:

$$Q_{conv} = hA\Delta T \quad (4)$$

$$Q_{cond} = k_h A \Delta T / \Delta z \quad (5)$$

$$Q_{rad} = \varepsilon \sigma A (T_{hot}^4 - T_{cold}^4) \quad (6)$$

In our case, the temperature difference of the laser copper block is  $\Delta T = 75 K$  (initial  $T_i = 298 K$  and final  $T_f = 223 K$  temperatures). The laser housing mass was  $0.25 kg$ , the time  $t = 900 s$  and  $c_p = 390 J kg^{-1} K^{-1}$ . Using the Equation 2., the heat transferred from the laser housing can be found as  $Q_{mass} = 8.1 W$ .

For still air heat transfer coefficient of free convection is  $h = 10 W m^{-2} K^{-1}$  and thermal conductivity  $k = 26,3 \times 10^{-3} W m^{-1} K^{-1}$  at  $1 atm$  and  $298 K$ ,  $\varepsilon = 1$  for black body radiation,  $\sigma = 5.6703 \times 10^{-8} W m^{-2} K^{-4}$  Stefan-Boltzmann constant. Exposed surface area of the laser housing  $A = 6,5 \times 10^{-3} m^2$  and thickness of the medium  $\Delta z = 0.15 m$ . The active heat load  $Q_{act}$  comes from the laser diode which is less than  $0.15 W$  and only  $0.05 W$  turn in to thermal energy in the laser diode.

When the system is operated at the vacuum condition that is about  $28 mBar$  the thermal conductivity of the air will be reduced to  $k_v = 4.5 \times 10^{-3} W m^{-1} K^{-1}$ . Heat transfer coefficient is proportional to the thermal conductivity. Accordingly the heat transfer coefficient in the vacuum chamber can be calculated as  $h_v = 1.612 W m^{-2} K^{-1}$ . The details of those calculations can be traced with the references [22, 23]. From the Equations 4., 5. and 6. the passive heat loads were calculated as  $Q_{conv} = 0.544 W$ ,  $Q_{cond} = 0.0015 W$ ,  $Q_{rad} = 0.00167 W$  respectively. Consequently, the total heat load on the system is  $Q_{load} = 0.66 W$ .

If the laser system were operated in the atmospheric condition the heat load would be  $3.522 W$  and for such reduction a  $14 cm$  thick isolation material with thermal conductivity of  $0.04 W m^{-1} K^{-1}$  is needed. Moreover, in the vacuum condition the humidity inside the chamber is reduced to well below  $\% 1$  relative humidity. This also helps the operation of the system due to huge heat capacity of water ( $4186 J kg^{-1} K^{-1}$ ) and condensation on the laser head and collimating optics.

## 2.4. Calculation of Cooling Power of A Cascade TEC System

Coefficient of performance is the ratio of the electrical to the cooling power of a TEC and it identifies the optimum current value for the best cooling performance. It is a critical issue since the higher values of current cause a detrimental effect on the cooling efficiency of the TEC by immediately appearing to be access energy and turning into heat. For a single TEC, COP value can be calculated as shown in Table 2. However, for a cascade system overall COP can be calculated as

$$\phi = \left[ \left( 1 + \frac{1}{\phi_s} \right)^N - 1 \right]^{-1} \quad (7)$$

where,  $\phi_s$  COP of a single TEC and  $N$  is the number of TECs [24]. Note that we assume all single TECs used have the same COP value. In general the maximum COP value is at about  $\leq 0.5I_{max}$  and that is the optimum conversion efficiency of the electrical power to the cooling power. By using Table 2. , the overall COP can be calculated as  $\phi \cong 0.05845$  and optimum conversion efficiency the cascade TEC system. This is approximately % 90 less than the TECs individual COP efficiency.

## 2.5. Maximum Allowable Thermal Resistance

The total heat dissipated by the hot side of the lower TEC ( $P_1$ ) is equal to heat produced by all TECs and plus cold side of the upper TEC ( $P_3$ ) cooling load. That is the thermal resistance of the heat sink to be used and it is given by

$$R_{hsmax} = \frac{T_{hot}-T_{amb}}{(VI)+Q_T} \quad (8)$$

where  $T_{hot}$  and  $T_{amb}$  are the temperatures belonging to hot side of the lower TEC and ambient and  $(VI)$  total electrical power applied to TECs. Regarding the optimum operational condition for the TECs (*i. e*  $\leq 0.5I_{max}$ ) the total electrical power applied was  $(VI) = 146.6W$ ,  $Q_T = 8.76W$ ,  $T_{hot} = 309K$  and  $T_{amb} = 298K$ . From those values the maximum allowable heat sink resistance of the system is found to be  $R_{hsmax} = 0.06962KW^{-1}$ . In other words, for a satisfactory heat transfer and so achieving desired cooling on the laser housing the thermal resistance of the heat sink to be used must be lower than  $R_{hsmax}$ .

## 2.6. Calculation Thermal Resistance of Heat Sink

For a successful ultra-cold laser system operation, the heatsink used has to meet heat resistance requirements that evacuate as fast as possible as the heat loads calculated above (Equation 8). The heatsink resistance strictly depends on the heatsink parameters. In order to achieve an accurate estimation meeting the requirements, a calculation procedure was constructed as shown in Table 4. Relatedly the input parameters that contains the specifications of the heat sink and air properties are given in Table 5. The calculations procedure has four major steps, including; the heatsink resistance prime area ( $A_t$ ), the forced air heat transfer coefficient ( $h$ ), overall surface efficiency ( $\eta_0$ ) and heatsink resistance ( $R_{hs}$ ).

**Table 4.** Table of the heatsink thermal resistant calculation

	Nomenclature	Formulas	Result
<b>Heatsink Prime Area Calculation (<math>A_f</math>)</b>			
	$b$ = Spacing between Fins ( $m$ )	$b = \frac{W - Nt}{N - 1}$	0.00967
	$A_c$ = Fin Cross-sections area ( $m^2$ )	$A_c = tL$	0.0012
	$P$ = Fin perimeter ( $m$ )	$P = 2t + 2L$	0.6080
	$A_f$ = Fin surface area ( $m^2$ )	$A_f = 2HL$	0.0390
	$A_b$ = Area between fins ( $m^2$ )	$A_b = (N-1)bL$	0.0408
	$A_t$ = Prime Area ( $m^2$ )	$A_t = NA_f$	0.6648
<b>Calculation of average heat transfer coefficient for forced air (<math>h</math>)</b>			
	$v$ = Volumetric flow rate of heatsink fan ( $m^3/s$ )	600 cfm = 0.284 $m^3/s$	0.284
	$V$ = Air velocity between fins ( $m/s$ )	$V = \frac{v}{NbH}$	30.119
	$Pr$ = Prandtl number of air at 1atm and 298 K	$Pr = \frac{C_p \mu}{K}$	0.704
	$Re$ = Reynolds Number	$Re = \frac{\rho V b}{\mu}$	17236.5
	$Re^*$ = Channel Reynolds number	$Re^* = Re \frac{b}{L}$	520.93
	$Nu_i$ = Ideal Nusselt's number	$Nu_i = \left[ \frac{1}{\left( \frac{Re^* Pr}{2} \right)^3} + \frac{1}{\left( 0.664 \sqrt{Re^*} Pr^{0.33} \sqrt{1 + \frac{3.65}{\sqrt{Re^*}}} \right)^3} \right]^{-1/3}$	14.54
	$h$ = Average heat transfer coefficient ( $W/m K$ )	$h = Nu_i \frac{K}{b}$	42.17
<b>Calculation of overall surface efficiency (<math>\eta_0</math>)</b>			
	$m$ = Fin parameter ( $1/m$ )	$m = \sqrt{\frac{hP}{k_{Al} A_c}}$	10.34
	$\eta_f$ = Fin efficiency	$\eta_f = \frac{\tanh(mH)}{mH}$	0.8725
	$\eta_0$ = Overall surface efficiency	$\eta_0 = 1 - \frac{NA_f}{A_t} (1 - \eta_f)$	0.8803
<b>Calculation of heat sink thermal resistance (<math>R_{hs}</math>)</b>			
	$R_{hs}$ = Thermal resistance of Heatsink ( $K/W$ )	$R_{hs} = \frac{1}{\eta_0 h A_t}$	0.04805

In the final step, the heat sink resistance  $R_{hs}$  found was compared with  $R_{hsmax}$  that was calculated based on the total heat load of the system using the Equation 8. Until reaching a satisfactory value for  $R_{hs}$  (i.e.  $R_{hs} < R_{hsmax} = 0.06962KW^{-1}$ ) heatsink parameters were iteratively changed. The final result was found as  $R_{hs} = 0.04805KW^{-1}$ . The calculation procedure was achieved with the aid of a commercial software (Mathematica 5.2). The detailed explanation about the formulas can be traced with the references [25, 26].

**Table 5.** Table of the heatsink specs and properties of air at 1atm and 28°C

Nomenclature (unit)	Values
<b>Heatsink Parameters</b>	
$H$ = Fin height (m)	0.065*
$L$ = Fin length (m)	0.3*
$W$ = Heatsink Width (m)	0.2*
$t$ = Fin Thickness (m)	0.004*
$N$ = Number of Fins	16
$K_{Al}$ = Fin thermal conductivity ( $Wm^{-1} K^{-1}$ )	200 **
<b>Properties of Air at 1atm and 27 °C</b>	
$\mu$ = Dynamic viscosity ( $kgm^{-1}s^{-1}$ )	$1.846 \times 10^{-7}$ **
$k$ = Thermal conductivity ( $kWm^{-1} K^{-1}$ )	$26.31 \times 10^{-6}$ **
$P$ = Mass Density ( $kgm^{-3}$ )	1.1614 **
$C_p$ = Specific heat ( $kJ kg^{-1} K^{-1}$ )	1.007 **

(\*) Measured, (\*\*) Ref. [27].

### 3. RESULTS

The other ultra-cold designs tabulated in Table 1. in the introduction section (i.e. [4], [5], [19], [20], [21]) reported their designs indicating that for a specific use rather than performance. Mostly their design concentrated on particular atomic transition that is not covered by the readily available coherent sources. Only Ref. [19] reveals calculations belonging to the TECs used in the cooling system. Therefore, we are only going to give calculation that leads to simulation process and performance measurement of contracted design of our system without involving in any comparison.

Since, the system is air cooled the environment temperature critically important. Heat transfer tests on the system were conducted at 25°C to identify the best environment temperature. (Figure 3) shows the graphs of the laser housing versus platform temperatures. The temperatures belonging the hot and cold sides of the TECs and heatsink were conducted by a computer controlled USB interface four channel thermometer (DT-8891E). Four *K-type* thermocouple sensor were placed to the holes on the heat diffusers located between the TEC modules and the heat sink. The temperature readings on the laser housing were achieved by the thermal sensor AD590JF located between the diode laser tube hole and bottom surface of the housing. The sensor was connected to the current controller (Thorlabs ITC 510) driving laser diode and top TEC. For both tests the air inside the system was evacuated down to 28mbar ensuring that the relative humidity is lower than 5 %. The upper TEC ( $P_3$ ) was started cooling the laser housing while the fans blowing  $380m^3/h$  air to the flaps. When  $P_3$  was reached about +15°C (or lower) it was switched off. This procedure allows faster cooling and using the heatsink reserve more efficiently. Then the middle and lower TECs were powered by the external power supply. The combination of TECs cooled the housing down to -35°C. The current applied was 7.95A corresponding to 17V for the maximum temperature difference. Finally, the top TEC was switched on and the laser housing reached

-50°C or lower temperatures. This procedure is valid when the room temperature is 25°C. However, when environment temperature was 20°C the process relatively faster and the housing temperature was able to be reached down to than -55°C. But, due to temperature controlling range of ITC 510 is limited with -50°C the data taken is considered in this range.

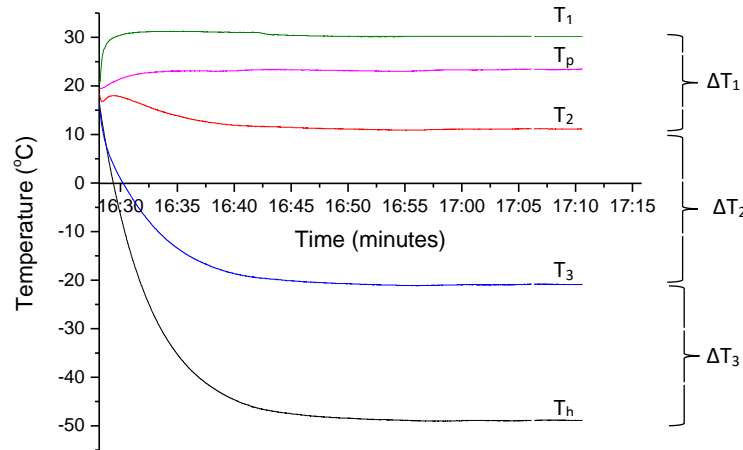


**Figure 3.** The graphs TECs temperature vs time;  $T_1$  = hot side temperature of the lower TEC  $P_1$ ,  $T_p$  = platform temperature,  $T_2$  = cold side temperature of the lower TEC ( $P_1$ ) and hot side temperature of the middle TEC ( $P_2$ ),  $T_3$  = hot side temperature of the upper TEC ( $P_2$ ) and hot side temperature of the middle TEC ( $P_3$ ),  $T_h$  = cold side temperature of the middle TEC ( $P_3$ ) and laser housing. The temperature differences are  $\Delta T_1 = T_2 - T_1$ ,  $\Delta T_2 = T_2 - T_3$ ,  $\Delta T_3 = T_3 - T_h$ .

### 3.1. Temperature-wavelength Tuning Enhancement

The temperature tuning range of the ECDL system was carried out using an AlGaInP type laser diode central wavelength 658nm at 25°C with an output power of 90mW at 135mA maximum current (Hitachi HL6535MG). Wavelength tunings limits of the laser diode was examined between -50°C and +60°C which are the extremum values for the platform and for the laser diode used. In (Figure 4a), temperature versus wavelength tuning of the 658nm laser is seen. During the measurement process the laser driver current was set to 135mA that was the maximum current for HL6535MG. The wavelength reading was conducted by a computer controlled fibre optical spectrometer (Thorlabs SPx-USB). The laser output power reading also recorded by an optical power meter with RS232 serial port computer connection (Thorlabs PM100). The power meter sensor was silicon based and has the spectral range of 400nm-1100nm with 5nW to 500mW optical power range. The minimum wavelength was 650.9nm at -50°C and after this point laser current was reduced gradually down to 39mA corresponding to 649nm with 3,5mW power (Figure 4b). In total it is possible to obtain 18.9nm tuning range between 3.5mW and 90mW output power (Figure 4c). The threshold current reduced to 35mA from 52mA by decreasing the case temperature from 298K to 223K. That is also contribution the output power and compensates the diffraction grating losses.

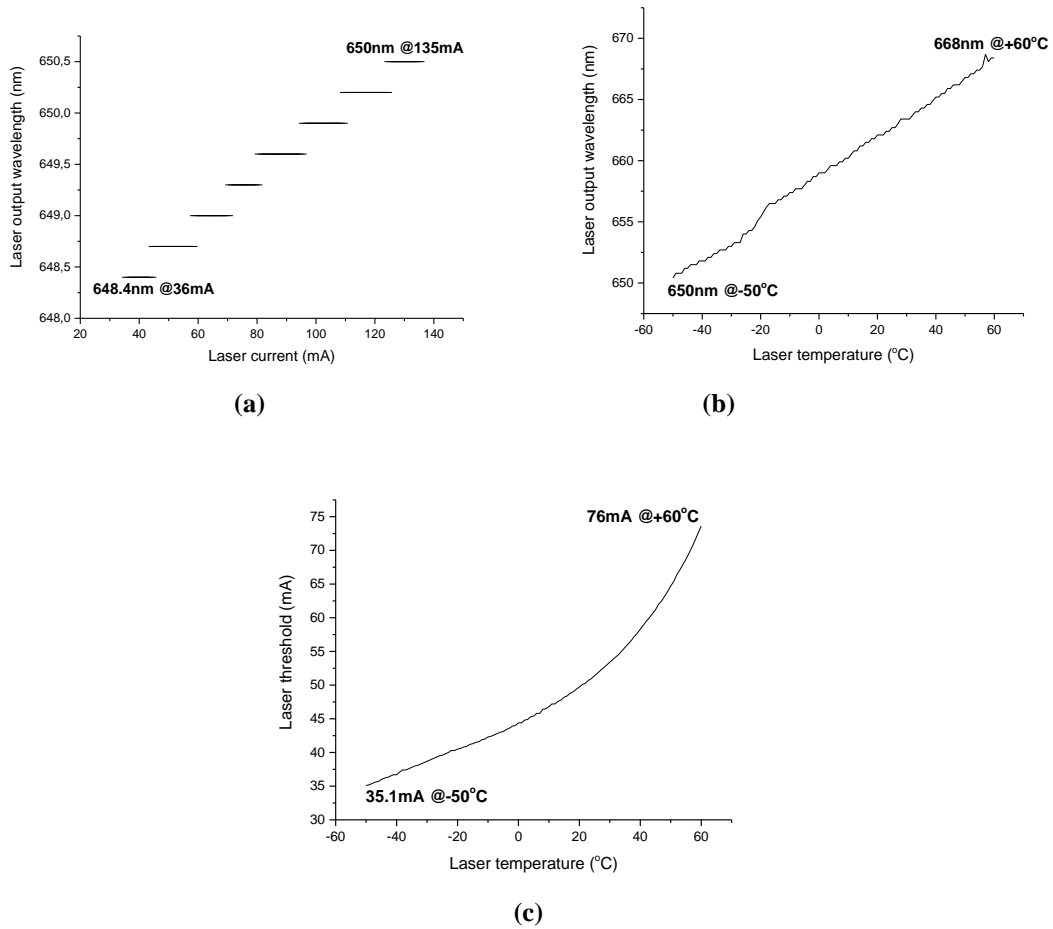


**Figure 4.** (a) The graph of HL6535MG 658nm laser diode temperature vs. laser wavelength, (b) Diode laser current and wavelength at 223K and (c) Lasing threshold current vs laser diode case temperature

### 3.2. Bandwidth Measurement

In (Figure 5) the bandwidth measurements of the laser at 298K and 223K are given. The test was conducted with a scanning Fabry-Perot Interferometer (FPI) set up. The FPI system was composed of a Thorlabs SA200-5B interferometer, a Thorlabs SA-201 controller and a GW-GDS 800 digital storage oscilloscope. The interferometer unit has 1.5GHz free spectral range (FSR), with 379 calculated finesse and 7MHz resolution. As shown in (Figure 5a) the room temperature linewidth of the laser is measured as 15MHz. Whereas the linewidth was halved by the reduction of the housing temperature from 298K to 223K (Figure 5b). The linewidth reduction with decreasing temperature comes from linewidth enhancement factor  $\alpha$  (also called Henry or  $\alpha$  factor) which is smaller for lower temperatures. The measurement shows that the linewidth is  $\leq 7\text{MHz}$  (estimating  $\approx 5\text{MHz}$ ) which was the minimum value for our device.

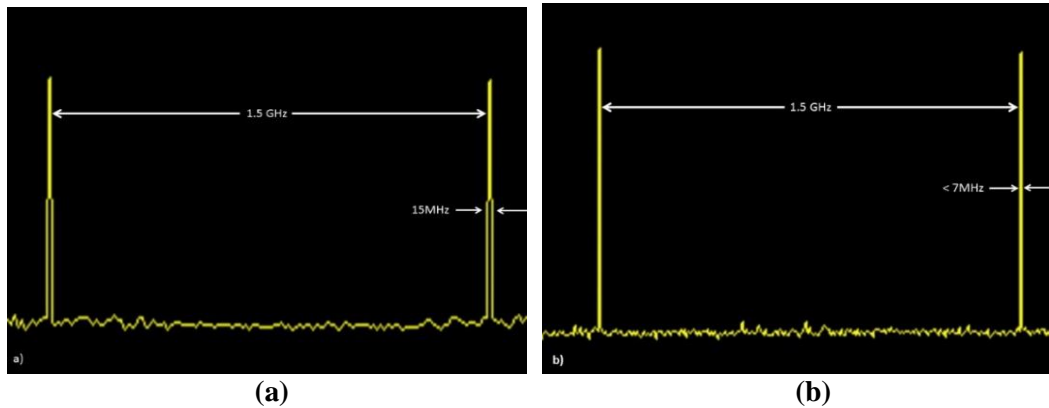


**Figure 5.** Band width measurement of external cavity with F-P etalon: (a) at 298K and (b) 223K

#### 4. CONCLUSION

The main motivation on this work was enhancing the spectral tuning range of an ECDL system with a practical way while narrowing the linewidth of the output beam. For this purpose, an ultra-cold vacuum ECDL system was designed and constructed. The laser system is capable of running at  $-50^{\circ}\text{C}$  (223K) under 28mBar vacuum. Running the system at very low temperatures under vacuum brings twofold wavelength scan range without thermal isolation. Other benefits are; the lower temperature reduces quantum noise resulting narrow linewidth and lower acoustic noise.

In order to identify specifications of the system components, a theoretical procedure was arranged. The formulation was converted to codes to calculate various parameters for optimum parameters for cooling of the laser housing and heat sink to evacuate the heat dissipated. Total cooling capacity and heat loads of the TECs, thermal resistance of the heat sink, thermal isolation of the vacuum system and air cooled heat evacuation rate were calculated. Accordingly, a heat sink was modified to serve as a platform for laser housing and a mounting platform for the external cavity FSE and other optics. The platform was also modified to attach a vacuum chamber and for an air cooling fan to evacuation heat dissipated. A TEC cooled laser diode housing and transmission diffraction grating was mounted on the platform having a vacuum enclosure on its top. The acrylic enclosure for vacuum achieved keeping the laser housing at the temperature of 223K and at pressure of 28mBar.

The design and construction stage was followed some performance tests and measurements. The measurements were mainly focused on heat transfer and vacuum performance of the platform, temperature wavelength tuning, threshold current variation, bandwidth for various temperatures between 298K temperature to 223K. The temperature tuning performance of the system was tested with 658nm laser diode below the room temperature 223K. We have seen that temperature tuning range of the can be enhanced almost two fold (about 18nm in total) while the line width reduced to half (7MHz or less) at 223K.

#### 5. DISCUSSION

Calculations showed that the laser system designed may be improved with some modifications on the platform and TEC configurations. Higher vacuum and the TECs with higher COP values in various combinations, accessing to lower laser diode case temperature is possible. That would allow wider temperature tuning range and narrower the linewidth via lesser quantum noise. Also the fan forced heat evacuation may be eliminated by increasing total fin area and replacing the aluminium fins with copper ones. Cancelling the fans will help the reduction on the mechanical noise and making the devise simpler.

## **ACKNOWLEDGEMENTS**

Thanks to Mersin University Department of Scientific Research Project via Research Project No: BAP-FBE FB (BP) 2014-1 YL.

## **CONFLICT OF INTEREST**

The authors stated that there are no conflicts of interest regarding the publication of this article.

## **REFERENCES**

- [1] Wieman CE, Holberg L. Using diode lasers for atomic physics. *Review of Scientific Instruments*. 1991; 62: 1-20.
- [2] Galbacs G. A review of applications and experimental instruments related to diode laser atomic spectroscopy. *Applied Spectroscopy Reviews*. 2006; 41: 259-303.
- [3] Affolderbach C, Milette G. A compact laser head with high-frequency stability for atomic Rb clocks and optical instruments. *Review of Scientific Instruments*. 2008; 79: 1-5.
- [4] Nguyen AT, Wang LB, Schauer MM, Torgerson JR. Extended temperature tuning of an ultraviolet diode laser for trapping and cooling single Yb<sup>+</sup> ions. *Review of Scientific Instruments*. 2010; 81: 053110.
- [5] Cozijn FMJ, Biesheuvel J, Flores AS, Ubachs W, Blume G, Wicht A, Paschke K, Erbert G, Koelemeij JCJ. Laser cooling of beryllium ions using frequency-doubled 626nm diode laser. *Optics Letters*. 2013; 38 (13): 2370-2372.
- [6] Ying K, Niu Y, Chen D, Cai H, Qu R, Gong S. White light cavity via modification of linear and nonlinear dispersion in N-type atomic system. *Optics Communications*. 2015; 342: 189-192.
- [7] Zhao YN, Zhang J, Stuhler J, Schuricht G, Lison F, Lu ZH, Wang LJ. Sub-Hertz frequency stabilisation of commercial diode laser. *Optics Communications*. 2010; 283: 4696-4700.
- [8] Fleming MW, Mooradian A. Spectral characteristics of external-cavity controlled semiconductor lasers. *IEEE Journal of Quantum Electronics*. 1981; QE-17 (1): 44-59.
- [9] Arnold AS, Wilson JS, Boshier MG. A simple extended-cavity diode laser. *Review of Scientific Instruments*. 1997; 69 (3): 1236-1239.
- [10] Loh H, Lin Y, Teper I, Cetina M, Simon J, Thompson JK, Vuletic V. Influence of grating parameters on the linewidths of external-cavity diode lasers. *Applied Optics*. 2006; 45 (36): 9191-9197.
- [11] Horstjann H, Nenakhov V, Burrows JP. Frequency stabilisation of blue extended cavity diode lasers by external cavity optical feedback. *Applied Physics B*. 2012; 106: 261-266.
- [12] Thomson DJ, Scholten RE. Narrow linewidth tuneable external cavity diode laser using wide bandwidth filter. *Review of Scientific Instruments*. 2012; 83: 023107.

- [13] Mroziejewicz B, Kowalczyk E, Dobrzanski L, Ratajczak J, Lewandowski SJ. External cavity diode lasers with E-beam silicon diffraction gratings. *Optical and Quantum Electronics*. 2007; 39: 585-595.
- [14] Hieta T, Vainio M, Mouser C, Ikenon E. External cavity lasers based a volume holographic grating at normal incidence for spectroscopy n the visible range. *Optics Communications*. 2009; 282: 3119-3123.
- [15] Bennets S, Hardman KS, Debs JE, McDonald GD, Kuhn CCN, Close JD, Robins NP. External cavity diode lasers with 5kHz linewidth and 200nm tuning range at 1.55 $\mu$ m. *Optics Express*. 2014; 22: 10643-10654.
- [16] Chuang C, Liao Y, Lin C, Chen S, Grillot F, Lin F. Linewidth enhancement factor in semiconductor lasers subject to various external optical feedback conditions. *Optics Express*. 2014; 22 (5): 5651-5658.
- [17] Tombez L, Cappelli F, Schilt S, Di Domenico G, Bartalini S, Hofstetter D. Wavelength tuning and thermal dynamics of continuous-wave mid-infrared distributed feedback quantum cascade lasers. *Applied Physics. Letters*. 2013; 103 (3): 1-5.
- [18] Dutta S, Elliott DS, and Chen YP. Mode-hop free tuning over 135 GHz of external cavity diode lasers without antireflection coating. *App. Phys. B*. 2012; 106: 629-633.
- [19] Fletcher CS, Close JD. Extended temperature tuning of an external cavity diode laser. *Applied Physics B*. 2014; 78: 305-313.
- [20] Ball H, Lee MW, Gensemer SD, Biercuk MJ. A high-power 626 nm diode laser system for beryllium ion trap. *Review of Scientific Instruments*. 2013; 84: 113104.
- [21] Tobias WG, Rosenberg JS, Hurtzler RN. A low-temperature external cavity diode laser for broad wavelength tuning. *Review of Scientific Instruments*. 2016; 87: 113104.
- [22] Incopera FP, Dewitt DP, Bergman TL. *Fundamentals of heat and mass transfer*. 6<sup>th</sup> ed. New York, NY, USA: Wiley, 2016; 152-155.
- [23] Welch K. *Capture Pumping Technology* 2<sup>nd</sup> Ed. Elsevier. 2001; 15-16.
- [24] Goldsmid HJ. *Introduction to Thermoelectricity*. London, LDN, UK: Heidelberg Dordrecht Springer, 2010; 1-3.
- [25] Teertstra P, Yovanovich MM, Culham JR. Analytical forced convection modelling of plate fin heat sinks. *Journal of Electronics Manufacturing*. 2001; 10 (4): 253-26.
- [26] Adeyanju AA, Compton W. Theoretical determination of a thermoelectric module heatsinks sizing. *International Journal of Electrical and Power Engineering*. 2010; 4 (2): 66-72.
- [27] Engineering tool box, [http://www.engineeringtoolbox.com/dry-air-properties-d\\_973.html](http://www.engineeringtoolbox.com/dry-air-properties-d_973.html)